

Solution of a Parabolic Partial Differential Equation on Digital Spaces: A Klein Bottle, a Projective Plane, a 4D Sphere and a Moebius Band

Alexander V. Evako

Laboratory of Digital Technologies, Moscow, Russia

Email address:

evakoa@mail.ru

To cite this article:

Alexander V. Evako. Solution of a Parabolic Partial Differential Equation on Digital Spaces: A Klein Bottle, a Projective Plane, a 4D Sphere and a Moebius Band. *International Journal of Discrete Mathematics. Advances in Materials*. Vol. 1, No. 1, 2016, pp. 5-14.

doi: 10.11648/j.dmath.20160101.12

Received: October 8, 2016; **Accepted:** November 17, 2016; **Published:** December 27, 2016

Abstract: This paper studies a parabolic partial differential equation on digital spaces and digital n-dimensional manifolds, which are digital models of continuous n-manifolds. Conditions for the existence of solutions of equations are determined and investigated. Numerical solutions of the equation on a Klein bottle, a projective plane, a 4D sphere and a Moebius strip are presented.

Keywords: Digital Surface, Graph, Parabolic PDE, Digital Topology, Moebius Strip, Klein Bottle, Projective Plane

1. Introduction

In the past decades, non-orientable surfaces such as a Moebius strip, Klein bottle and projective plane have attracted many scientists from different fields. The study was derived from obvious practical and science background. In physics, a considerable interest has emerged in studying lattice models on non-orientable surfaces as new challenging unsolved lattice-statistical problems and as a realization and testing of predictions of the conformal field theory (see, e.g., [13]). In a joint Russian-French-German project a Moebius strip was proposed as a basic element of an airplane wing. Many important technical and physical properties of Moebius-type structural elements can be described by solutions of partial differential equations (PDE), where a Moebius strip serves as a domain. A problem exists in description of electronic and nuclear motions in nano-technology structures and biological networks. Modeling blood flow through a capillary network or road traffic requires a system of differential equations on a graph. Since analytic solutions of PDE can be obtained only in simple geometric regions, for practical problems, it is more reasonable to use computational or numerical solutions. We can do this by implementing as domains graphs and digital spaces, which are discrete counterparts of continuous spaces, and by transferring PDE from a continuous area into discrete

one. A review of works devoted to partial differential equations on graphs can be found in [2], [14], and [17]. A serious problem arises because in most of cases, the grid is not a correct counterpart of the continuous area in terms of digital topology and, therefore, cannot properly model the continuous domain. Distinctions between the differential equations on discrete and continuous spaces are also essential. One of differences is stipulated by the fact that a digital space can have just a few points. Another serious difference is linked to the existence of the natural least length in a digital space, defined by the length of the edge connecting two adjacent points of the space. In application to wave processes it means a lack of indefinitely short waves and indefinitely high frequencies that is the lack of the factors frequently conducting to divergences.

In order to build mathematically correct grids it is reasonable to use digital topology methods.

Digital spaces are studied in the framework of digital topology, which plays an important role in analyzing n-dimensional digitized images arising in computer graphics as well as in many areas of science including neuroscience, medical imaging, computer graphics, geoscience and fluid dynamics. Usually, digital objects are represented by graphs whose edges define nearness and connectivity (see, e.g., [3] and [6]). The important feature of an n-surface is a similarity of its properties with properties of its continuous counterpart

in terms of algebraic topology. For example, the Euler characteristics and the homology groups of digital n-spheres, a Moebius strip and a Klein bottle are the same as ones of their continuous counterparts ([10] and [11]). In recent years, there has been a considerable amount of works devoted to building two, three and n-dimensional discretization schemes and digital images. In papers [4] and [9], discretization schemes are defined and studied that allow to build digital models of 2-dimensional continuous objects with the same topological properties as their continuous counterparts.

Section 2: The material to be presented below begins with a short description digital spaces and digital n-surfaces studied in [5], [6], [8] such as digital n-dimensional spheres, a digital torus, a digital Klein bottle, etc.

Section 3 defines parabolic differential equations on a digital space and a network and studies some its properties.

Section 4 presents a numerical solution of a parabolic equation on a digital Klein bottle, a digital projective plane, a digital 4D sphere, a digital Moebius band and a directed network installed in digital space (which, for example, can model a capillary network for blood flow).

2. Digital N-surfaces

There are a considerable amount of literature devoted to the study of different approaches to digital lines, surfaces and spaces in the framework of digital topology. Digital topology studies topological properties of discrete objects which are obtained digitizing continuous objects.

This section includes some results related to digital spaces. Traditionally, a digital image has a graph structure (see [3] and [7]). A digital space G is a simple undirected graph $G=(V, W)$ where $V=(v_1, v_2, \dots, v_n, \dots)$ is a finite or countable set of points, and $W = ((v_p v_q), \dots)$ is a set of edges. Topological properties of G as a digital space in terms of adjacency, connectedness and dimensionality are completely defined by set W . Let G and v be a graph and a point of G . In [7], the subgraph $O(v)$ containing all neighbors of v (without v) is called the rim of point v in G . The subgraph $U(v)=v \cup O(v)$ containing $O(v)$ as well as point v is called the ball of point v in G . Let (vu) be an edge of G . The subgraph $O(vu)=O(v) \cap O(u)$ is called the rim of (vu) .

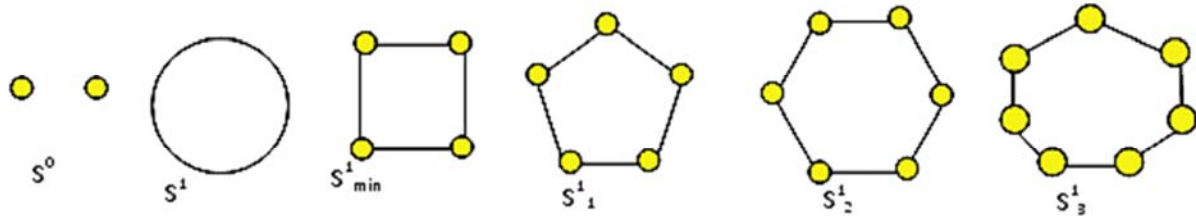


Fig. 1. S^0 is a digital zero-dimensional sphere, $S^1_{min}, S^1_1, S^1_2, S^1_3$ are digital one-dimensional spheres.

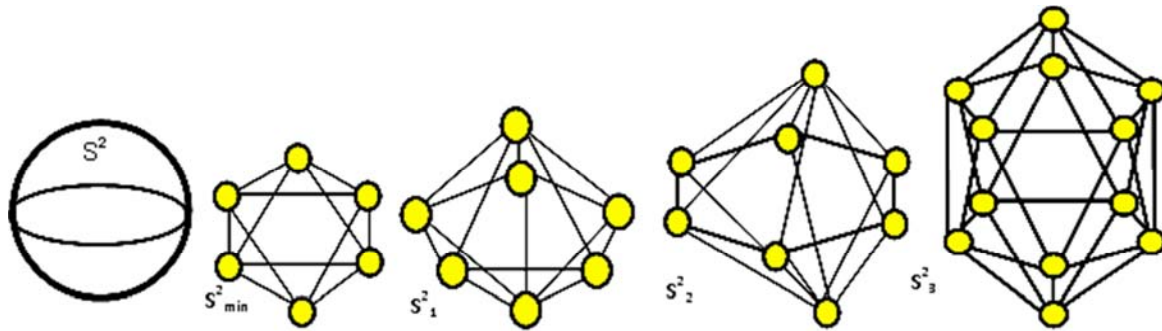


Fig. 2. Two-dimensional spheres with a different number of point, any of spheres can be converted into the minimal sphere S^2_{min} by contractible transformations.

For two graphs $G=(X, U)$ and $H=(Y, W)$ with disjoint point sets X and Y , their join $G \oplus H$ is the graph that contains G, H and edges joining every point in G with every point in H .

Contractible graphs are basic elements in this approach.

Definition 2.1

- A one-point graph is contractible. If G is a contractible graph and H is a contractible subgraph of G then G can be converted into H by sequential deleting simple points.
- A point v in graph G is simple if the rim $O(v)$ of v is a contractible graph.
- An edge (uv) of a graph G is called simple if the rim $O(vu)=O(v) \cap O(u)$ of (uv) is a contractible graph.

By construction, a contractible graph is connected. It follows from definition 1 that a contractible graph can be converted to a point by sequential deleting simple points.

Definition 2.2

- Deletions and attachments of simple points and edges are called contractible transformations.
- Graphs G and H are called homotopy equivalent if one of them can be converted to the other one by a sequence of contractible transformations.

Homotopy is an equivalence relation among graphs. Contractible transformations of graphs seem to play the same role in this approach as a homotopy in algebraic topology. In papers [10] and [11], it was shown that contractible

transformations retain the Euler characteristic and homology groups of a graph. A digital n-manifold is a special case of a digital n-surface defined and investigated in [6].

Definition 2.3

The digital 0-dimensional surface $S^0(a, b)$ is a disconnected graph with just two points a and b. For $n > 0$, a digital n-dimensional surface G^n is a nonempty connected graph such that, for each point v of G^n , $O(v)$ is a finite digital (n-1)-dimensional surface.

- A connected digital n-dimensional surface G^n is called a digital n-sphere, $n > 0$, if for any point $v \in G^n$, the rim $O(v)$ is an (n-1)-sphere and the space $G^n - v$ is a contractible graph.
- A digital n-dimensional surface G^n is a digital n-manifold if for each point v of G^n , $O(v)$ is a finite digital (n-1)-dimensional sphere.

Digital n-manifolds are called homeomorphic if they are

homotopy equivalent. A digital n-manifold M can be converted to a homeomorphic digital n-manifold N with the minimal number of points by contractible transformations.

Definition 2.4

- Let M be a digital n-sphere, $n > 0$, and v be a point belonging to M. The space $N = M - v$ is called a digital n-disk with the boundary $\partial N = O(v)$ and the interior $\text{Int}N = N - \partial N$.
- Let M be an n-manifold and a point v belong to M. Then the space $N = M - v$ is called an n-manifold with the spherical boundary $\partial N = O(v)$ and the interior $\text{Int}N = N - \partial N$.

According to definition 2.3, a digital n-disk is a contractible graph. A digital n-disk is a digital counterpart of a continuous n-dimensional disk in Euclidean E^n .

The following results were obtained in [6] and [8].

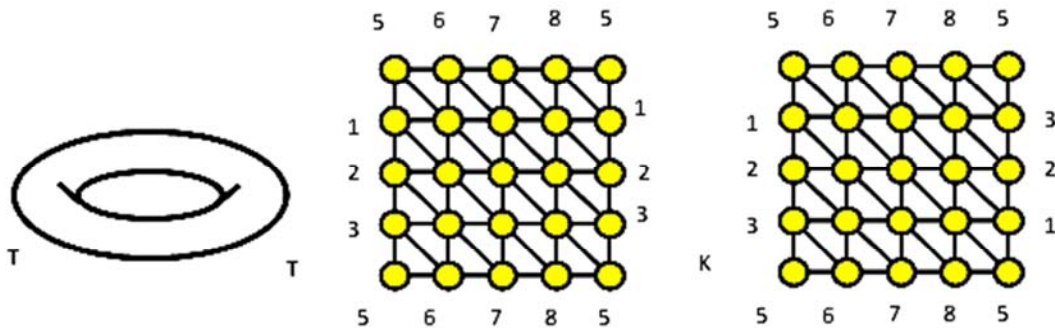


Fig. 3. Digital 2-dimensional torus T and Klein bottle K with sixteen points.

Theorem 2.1

- The join $S^n_{\min} = S^0 \oplus S^0_2 \oplus \dots \oplus S^0_{n+1}$ of (n+1) copies of the zero-dimensional sphere S^0 is a minimal n-sphere.
- Let M and N be n and m-spheres. Then $M \oplus N$ is an (n+m+1)-sphere.
- Any n-sphere M can be converted to the minimal n-

sphere S_{\min} by contractible transformations.

- Let M be an n-manifold, G and H be contractible subspaces of M and v be a point in M. Then subspaces $M - G$, $M - H$ and $M - v$ are all homotopy equivalent to each other.

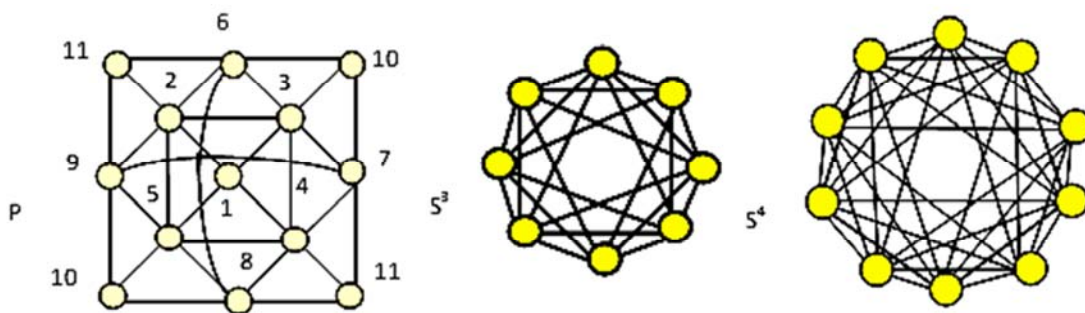


Fig. 4. P, S^3 and S^4 are digital two-dimensional projective plane, three- and four-dimensional spheres respectively.

The replacement of an edge with a point increases the number of points in a digital n-manifold.

Definition 2.5

Let M be an n-manifold, v and u be adjacent points in M and (vu) be the edge in M. Glue a point x to M in such a way that $O(x) = v \oplus u \oplus O(vu)$, and delete the edge (vu) from the space. This pair of contractible transformations is called the replacement of an edge with a point or R-transformation, $R: M \rightarrow N$. The obtained space N is denoted by $N = RM = (MUx) -$

(vu).

Theorem 2.2 ([8])

Let M be an n-manifold and $N = RM$ be a space obtained from M by an R-transformation. Then N is homeomorphic to M.

An R-transformation is a digital homeomorphism because it retains the dimension and other local and global topological features of an n-manifold. R-Transformations increase the number of points in a given n-manifold M

retaining the global topology (the homotopy type of M) and the local topology (the homotopy type and the dimension of the neighborhood of any point). A close connection between continuous and digital n -manifolds for $n=2$ was shown in [4].

A digital 0-dimensional surface is a digital 0-dimensional sphere. Fig. 1 depicts digital zero and one-dimensional spheres. Fig. 2 shows digital 2-dimensional spheres. All spheres are homeomorphic and can be converted into the minimal sphere S^2_{\min} by contractible transformations. Digital torus T and a digital 2-dimensional Klein bottle K are shown in fig. 3. Fig. 4 depicts a digital projective plane P and digital three and four-dimensional spheres S^3 and S^4 respectively. In the finite difference method for solving partial differential equations in two and three dimensions, a two or three-dimensional continuous domain is replaced by a grid. This grid has to be a digital model of a continuous space. However, in most of cases, the grid is not a correct two or three-dimensional space in terms of digital n -surfaces. For example, consider a standard two-dimensional grid G (fig. 5(a)) often used in finite-difference schemes. As one can see, the neighborhood $O(v)$ of any point v consists of four non-adjacent points and, therefore, is not a one-dimensional

sphere. Hence, G is not a part of a digital two-dimensional plane, but rather can be seen as a collection of one-dimensional segments. Grid H in fig. 5(c) is a part of a digital plane because the rim $O(v)$ of any interior point v is a digital 1-sphere S^1 containing six points and shown in fig. 1. Thus, H is a correct grid which should be used in finite-difference schemes.

3. Parabolic PDE on a Digital Space

3.1. The Structure of Parabolic Partial Differential Equations on a Digital Space

Some results of the investigation of partial differential equations on digital spaces were published in [5]. Finite difference approximations of the PDE are based upon replacing partial differential equations by finite difference equations using Taylor approximations [15]. Consider a parabolic PDE with two spatial independent variables.

$$\frac{\partial f}{\partial t} = a \frac{\partial^2 f}{\partial x^2} + b \frac{\partial^2 f}{\partial y^2} + g \quad (1)$$

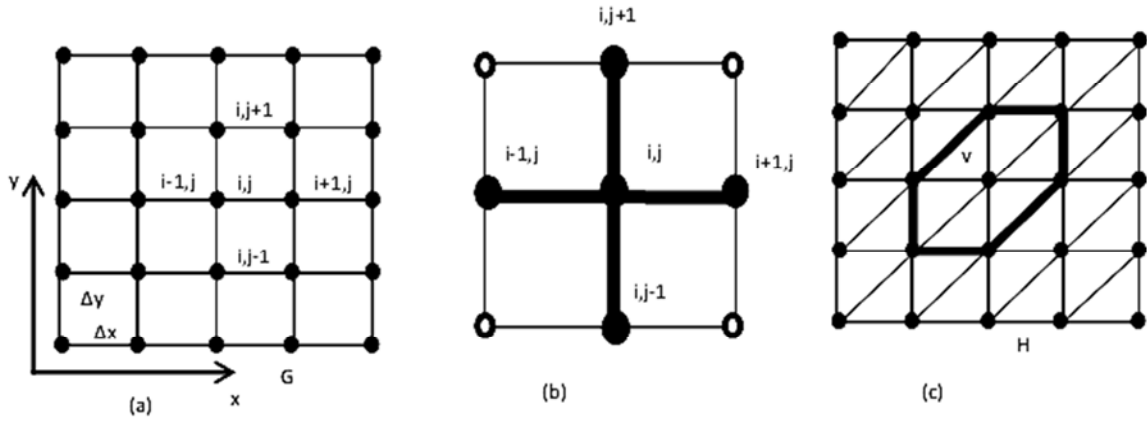


Fig. 5. (a) Finite difference 2D grid for two independent variable x and y , (b) The spatial stencil for the parabolic partial differential equation with two spatial independent variables x and y , (c) Digital 2-dimensional plane.

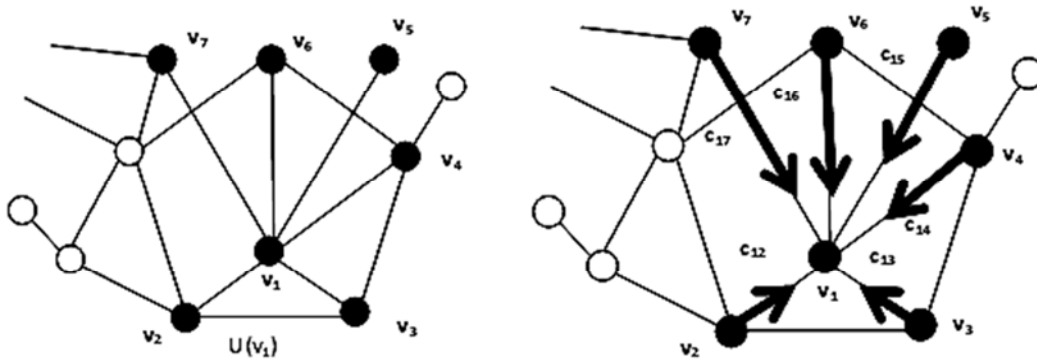


Fig. 6. The ball $U(v_1)$ of point v_1 (black points). $F_i^{t+1} = c_{11}^t f_i^t + c_{12}^t f_2^t + c_{13}^t f_3^t + c_{14}^t f_4^t + c_{15}^t f_5^t + c_{16}^t f_6^t + c_{17}^t f_7^t$.

where $f = f(x, y, t)$, $a = a(x, y, t)$, $b = b(x, y, t)$, $g = g(x, y, t)$. Using a two-dimensional spatial orthogonal grid G shown in fig. 5(a), the central difference formula for the second derivatives with respect to x and y , and the forward difference formula for the derivative with respect to t , we obtain the following equivalent finite difference equation

$$\frac{f_{i,j}^{n+1} - f_{i,j}^n}{\Delta t} = a_{i,j}^n \frac{f_{i-1,j}^n - 2f_{i,j}^n + f_{i+1,j}^n}{\Delta x^2} + b_{i,j}^n \frac{f_{i,j-1}^n - 2f_{i,j}^n + f_{i,j+1}^n}{\Delta y^2} + g_{i,j}^n \quad (2)$$

where $x = i\Delta x, i = 1, 2, \dots, y = j\Delta y, j = 1, 2, \dots, t = n\Delta t, n = 1, 2, \dots$. Equation (2) can be written as

$$f_{i,j}^{n+1} = e_{i-1,j}^n f_{i-1,j}^n + e_{i+1,j}^n f_{i+1,j}^n + e_{i,j-1}^n f_{i,j-1}^n + e_{i,j+1}^n f_{i,j+1}^n + e_{i,j}^n f_{i,j}^n + \Delta t g_{i,j}^n \tag{3}$$

where $e_{i,j}^n = 1 - e_{i-1,j}^n - e_{i+1,j}^n - e_{i,j-1}^n - e_{i,j+1}^n$, $e_{i-1,j}^n = e_{i+1,j}^n = \frac{\Delta t}{\Delta x^2} a_{i,j}^n$, $e_{i,j-1}^n = e_{i,j+1}^n = \frac{\Delta t}{\Delta x^2} b_{i,j}^n$.

Grid G in fig. 5(a) is a graph with points $v_{ps} = (p\Delta x, s\Delta y)$. Point v_{ij} is adjacent to points $v_{i,j\pm 1}$ and $v_{i\pm 1,j}$. Notice that points $v_{ij}, v_{i,j\pm 1}$ and $v_{i\pm 1,j}$ form the ball $U(v_{ij}) = v_{ij} \cup O(v_{ij})$ depicted in fig.5(b). Based on this consideration and equation (3), we can define a dynamic system on a digital space G by the set of equations on G.

$$f_p^{t+1} = \sum_{v_k \in U(v_p)} c_{pk}^t f_k^t + g_p^t, p = 1, \dots, n, \text{ where } \sum_{v_k \in U(v_p)} c_{pk}^t = 1, p = 1, \dots, n \tag{4}$$

The summation is produced over all points v_k belonging to the ball $U(v_p)$ of point v_p . Here f_k^t is the value of the function $f(v_k, t)$ at point v_k of G at the moment t, coefficients c_{pk}^t are functions on the pairs of point (v_p, v_k) and t (with domain $V \times V \times t$). If points v_p and v_k are not adjacent, then $c_{pk}^t = 0$.

$$f_p^0 = f(v_p, 0), p = 1, 2, \dots, n \tag{9}$$

Definition 3.2

Equations (5) along with initial conditions (9) are called the initial value problem for the parabolic PDE on a digital space $G(v_1, v_2, \dots, v_n)$.

Remark 3.1

In general, the condition $\sum_{v_k \in U(v_p)} c_{pk}^t = 1, p = 1, 2, \dots, n$, is not necessary for the PDE. For example, it does not hold for the diffusion equation on a directed network. If all $g_p^t = 0$, then the equation is called homogeneous. Later on in this paper, all $g_p^t = 0$.

$$f_p^{t+1} = \sum_{v_k \in U(v_p)} c_{pk}^t f_k^t, f_p^0 = f(v_p, 0), p = 1, 2, \dots, n \tag{10}$$

Boundary conditions can also be set the usual way. Boundary conditions are affected by what happens at the subspace H of G. Let H be a subspace of G. Let the value of the function $f(v_k, t)$ at points $v_k \in H$ at the moment t be given by the set

$$f(v_k, t) = f_k^t = s_k^t, v_k \in H \tag{11}$$

The boundary-value problem on G can be formulated as follows

Definition 3.1

Let $G(V, W)$ be digital space (graph) with the set of points $V = (v_1, v_2, \dots, v_n)$, the set of edges $W = ((v_p, v_q), \dots)$, and $U(v_p)$ be the ball of point v_p . A parabolic PDE on G is the set of n equations of the form

$$f_p^{t+1} = \sum_{v_k \in U(v_p)} c_{pk}^t f_k^t, p = 1, \dots, n \tag{5}$$

Definition 3.3

Thus a PDE on a given point v_k depends on the values of a function on v_k and the points adjacent to v_k . Equation (5) is illustrated in fig. 6. The ball $U(v_1)$ consists of black points, and $f_1^{t+1} = c_{11}^t f_1^t + c_{12}^t f_2^t + c_{13}^t f_3^t + c_{14}^t f_4^t + c_{15}^t f_5^t + c_{16}^t f_6^t + c_{17}^t f_7^t$. Since $c_{pk}^t = 0$ if points v_p and v_k are non-adjacent, then set (5) can be written in the form

Let $G(v_1, v_2, \dots, v_n)$ be a digital space and the set (5) be a differential parabolic equation on G. Let H be a subspace of G, and the value of the function $f(v_k, t)$ at points $v_k \in H$ at the moment t be defined by boundary conditions (11). Equation (5) along with boundary conditions (11) is called the boundary value problem for the parabolic PDE on a digital space G.

$$f_p^{t+1} = \sum_{v_k \in U(v_p)} c_{pk}^t f_k^t = \sum_{k=1}^n c_{pk}^t f_k^t, p = 1, 2, \dots, n, \tag{6}$$

$$f_p^{t+1} = \sum_{v_k \in U(v_p)} c_{pk}^t f_k^t, p = 1, 2, \dots, n, f(v_k, t) = s_k^t, v_k \in H, \tag{12}$$

Equations (6) do not depend explicitly on the dimension of G and can be applied to a digital space of any dimension or a network. All dimensional features are contained in the local and global structure of a digital space G. Set (6) is similar to the set of differential equations on a graph investigated by A. I. Volpert in [16]. Equation (6) can be presented in the matrix form

Consider the stability of equation (5) using a standard approach. For f^t , the norm is defined as $\|f^t\| = |f_1^t| + \dots + |f_n^t|$. Equation (5) is called stable according to initial values if there exists a positive b such that $\|f^t\| \leq b \|f^0\|$, for all t.

$$f^t = \begin{bmatrix} f_1^t \\ \cdot \\ f_n^t \end{bmatrix}, C(t) = \begin{bmatrix} c_{11}^t & c_{12}^t & \cdot \\ c_{21}^t & \cdot & \cdot \\ \cdot & \cdot & c_{nn}^t \end{bmatrix}, \tag{7}$$

Theorem 3.1

An equation (10) on a digital space $G(v_1, v_2, \dots, v_n)$ is stable according to initial values, i.e., $\|f^t\| \leq M \|f^0\|$, if for any t there is $b, 0 < b < 1/n$, such that $|c_{pk}^t| \leq b, p, k = 1, \dots, n$.

$$f^{t+1} = C(t) f^t \tag{8}$$

Proof

Consider now the initial conditions for solving equation (5). Initial conditions are defined in a regular way by the set of equations

Consider the equation in form (6). $|f_p^{t+1}| = |\sum_{k=1}^n c_{pk}^t f_k^t| \leq \sum_{k=1}^n |c_{pk}^t| |f_k^t| \leq b \sum_{k=1}^n |f_k^t| = b \|f^t\|$. Then $\|f^{t+1}\| = |f_1^{t+1}| + \dots + |f_n^{t+1}| \leq b \|f^t\| + \dots + b \|f^t\| = bn \|f^t\| < 1/n n \|f^t\| = \|f^t\|$. Since $\|f^{t+1}\| < \|f^t\|$ for any t, then $\|f^t\| < \|f^0\|$. It completes the proof.

3.2. The Heat and Diffusion Equations

Later in this section we consider homogeneous equations. Diffusion is the process by which particles are transported from one point of a digital space $G(v_1, v_2, \dots, v_n)$ to another points adjacent to the first one as a result of random motions: the number $c_{pk}^t f_k^t$ of particles on point v_k will jump to point v_p , the number $c_{pp}^t f_p^t$ of particles on point v_p will stay on v_p .

$$f_p^{t+1} = \sum_{v_k \in U(v_p)} c_{pk}^t f_k^t, p = 1, 2, \dots, n, \sum_{v_p \in U(v_k)} c_{pk}^t = 1, c_{kp}^t \geq 0, k = 1, \dots, n \tag{14}$$

Let us show that the sum $S^t = \sum_{k=1}^n f_k^t$ of values of the function on all points of the digital space G for a diffusion equation (14) according to initial values does not depend on t.

Theorem 3.2

In the diffusion equation (14) on a digital space $G(v_1, v_2, \dots, v_n)$, the sum $S^t = \sum_{k=1}^n f_k^t$ of values of the solution f_p^t on all points of G according to initial values does not depend on t.

Proof

Consider the diffusion equation in the form (6). $S^{t+1} = \sum_{p=1}^n f_p^{t+1} = \sum_{p=1}^n \sum_{k=1}^n c_{pk}^t f_k^t = \sum_{k=1}^n \sum_{p=1}^n c_{pk}^t f_k^t =$

$$\|f^{t+1}\| = \sum_{p=1}^n |f_p^{t+1}| = \sum_{p=1}^n \left| \sum_{k=1}^n c_{pk}^t f_k^t \right| \leq \sum_{p=1}^n \sum_{k=1}^n |c_{pk}^t| |f_k^t| = \sum_{k=1}^n \sum_{p=1}^n |c_{pk}^t| |f_k^t| = \sum_{k=1}^n |f_k^t| \sum_{p=1}^n |c_{pk}^t|.$$

According to (13), $\sum_{p=1}^n |c_{pk}^t| = \sum_{p=1}^n c_{pk}^t = 1, k = 1, \dots, n$. Therefore, $\|f^{t+1}\| \leq \sum_{k=1}^n |f_k^t| = \|f^t\|$. Hence, $\|f^t\| \leq \|f^0\|$. The proof is complete. □

At rather large times t, the form of a solution will be determined by a limit form of a matrix $C^t = \prod_{s=0}^t C(s)$. It is of some interest to clarify a behavior of matrix C^t as $t \rightarrow \infty$. Call this limit as a final matrix C^∞ . The final matrix C^∞ converts initial values f_k^0 into final values f_k^∞ . In the diffusion equation (14) in the matrix form (8), the square (n x n)-matrix C^t is a stochastic matrix (or, more correct, a

Conservation of the total number of particles is obvious, i.e., $f_k^t = \sum_{v_p \in U(v_k)} c_{pk}^t f_k^t$. This means that

$$\sum_{v_p \in U(v_k)} c_{pk}^t = 1, c_{kp}^t \geq 0, k = 1, \dots, n, \tag{13}$$

Definition 3.4

Let $G(v_1, v_2, \dots, v_n)$ be a digital space and the set (5) be a parabolic PDE on G. If coefficients satisfy the set (13), then equation (5) is called the diffusion equation on a digital space G.

$\sum_{k=1}^n f_k^t \sum_{p=1}^n c_{pk}^t$. According to (13), $\sum_{p=1}^n c_{pk}^t = 1, k = 1, \dots, n$. Therefore, $S^{t+1} = \sum_{k=1}^n f_k^t = S^t$. Hence, $S^t = S^0$. The proof is complete.

It is easy to see that equation (14) is stable.

Theorem 3.3

A diffusion equation (14) on a digital space $G(v_1, v_2, \dots, v_n)$ is stable according to initial values, i.e., $\|f^t\| \leq \|f^0\|$, if for any t.

Proof

Consider the diffusion equation in the form (6).

transposed stochastic matrix) which properties are well known (see [1] and [12]). Such matrices are used in Markov processes. Let's consider some applications of such approach for a solution of the initial value problem for the diffusion equation on a digital space $G(v_1, v_2, \dots, v_n)$. Consider the case when matrix C(t) is not time dependent, $C(t) = C = \{c_{pk}\}$. Then the initial value problem for the diffusion equation on a digital space $G(v_1, v_2, \dots, v_n)$ is the set (14) when

$$C(t) = C = \{c_{pk}\}, c_{pk} \geq 0, p, k = 1, \dots, n \tag{15}$$

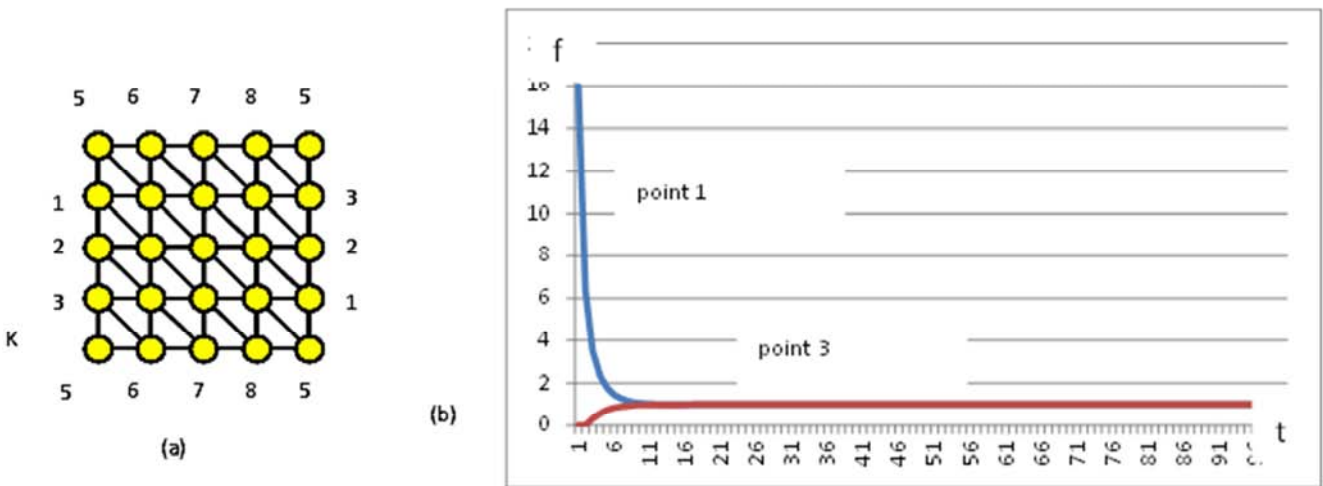


Fig. 7. (a) K is a digital Klein bottle containing 16 points. (b) The solution profile at point 1 and 3 on the Klein bottle K, $t=0, 1, \dots, 100, f_1^0=16, f_k^0=0, k \neq 1$.

If matrix C is indecomposable and primitive, then it has a simple maximum eigenvalue 1, and there are no other complex eigenvalues which modulus are equal one (see [1]

and [12]). Matrix C^t converges to a limit stochastic matrix C^∞ as $t \rightarrow \infty$, which can be presented in the following form:

$$C^\infty = \begin{bmatrix} c_1 & \cdot & c_1 \\ \cdot & \cdot & \cdot \\ c_n & \cdot & c_n \end{bmatrix} = \lim_{t \rightarrow \infty} (C(t) \times C(t-1) \dots \times C(0)), \sum_{k=1}^n c_k = 1, \forall c_k > 0. \tag{16}$$

Theorem 3.4

If matrix $C = \{c_{pk}\}$ in the diffusion equation (14) is indecomposable and primitive, then the final solution f^∞ of (14) as $t \rightarrow \infty$ at any initial values is stationary, not time-dependent (in each point of space, a value of function f^∞ is constant, does not depend on time t), is determined only by the sum of values of function f in all points of the space G and has the form:

$$f^\infty = C^\infty f^0 \tag{17}$$

$$f^\infty = S \begin{bmatrix} c_1 \\ \cdot \\ c_n \end{bmatrix}, C^\infty = \begin{bmatrix} c_1 & \cdot & c_1 \\ \cdot & \cdot & \cdot \\ c_n & \cdot & c_n \end{bmatrix}, f^0 = \begin{bmatrix} f_1^0 \\ \cdot \\ f_n^0 \end{bmatrix}, \sum_{k=1}^n f_k^0 = S, \sum_{k=1}^n c_k = 1, \forall c_k > 0 \tag{18}$$

Proof

$C^\infty = \lim_{t \rightarrow \infty} (C(t) \times \dots \times C(0))$. According to [1] and [12], $C^\infty = \begin{bmatrix} c_1 & \cdot & c_1 \\ \cdot & \cdot & \cdot \\ c_n & \cdot & c_n \end{bmatrix}$. It is easy to check directly that $C^\infty f^0 = f^\infty$ and $C f^\infty = f^\infty$. Therefore, f^∞ the final solution of (14). The proof is complete.

Clearly, the solution f^∞ depends only on S , but not on concrete distribution of values of function f^0 on points of space G in the initial moment $t = 0$. Besides, any function of the form $f = d f^\infty$ is an eigenvector of $C = C^0 = C^t$, and a stationary solution of the equation (13) because $C f = C C(\infty) f = C(\infty) C = f$. That is

$$f_p = \sum_{v_k \in G} c_{pk} f_k \tag{19}$$

This equation can be considered as an analog of an elliptical equation on a digital space.

The accuracy of the solution of equation (5) can be increased by several ways. The first way is to tune functions c_{pk}^t in (5) so that the accuracy is higher. This way is not the best because equation (5) must fit the given PDE and cannot be used for other equations. The other way is to use more points in the domain which is a digital space G . For example,

an edge (uv) in G can be replaced by a point z using contractible transformations, and the obtained space $(G - (uv)) \cup z$ is homeomorphic to G (see [8]). In fig. 2, digital 2-sphere S^2_{min} containing six points can be replaced by S^2_3 containing twelve points.

4. Numerical Solutions of a Diffusion Equation

Consider several examples of the numerical solutions of the diffusion equation (14) on different digital spaces.

$$f_p^{t+1} = \sum_{v_k \in U(v_p)} c_{pk} f_k^t = \sum_{k=1}^n c_{pk} f_k^t, p = 1, 2, \dots, n, \tag{20}$$

$$\sum_{p=1}^n c_{pk} = 1, c_{pk} \geq 0, k, p = 1, 2, \dots, n$$

4.1. Digital 2-dimensional Klein Bottle K . the Heat Equation on K

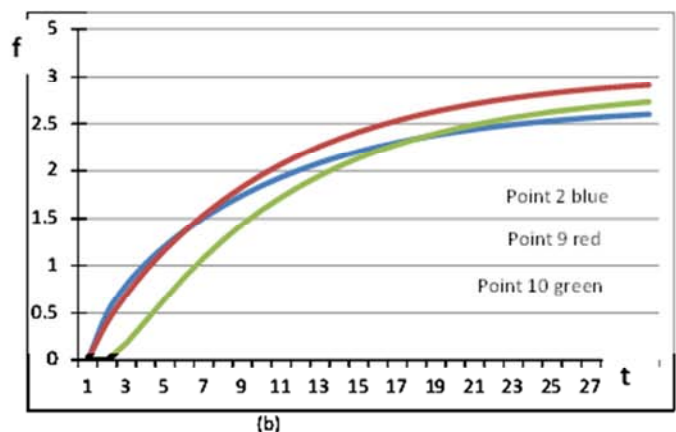
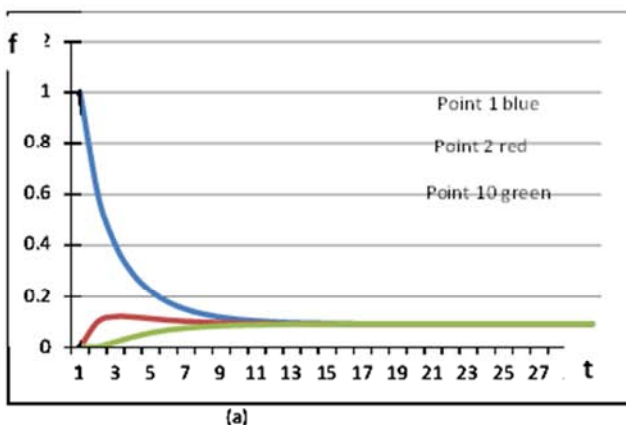


Fig. 8. Numerical solutions on the projective plane P . (a) The solution profile of the initial value problem at points 1, 2 and 10 on the projective plane P , $t=0, 1, \dots, 30, f_i^0=1, f_k^0=0, k \neq 1$. (b) The solution profile of the boundary value problem at points 2, 8 and 11 on the Moebius strip M , $t=0, 1, \dots, 30, f_i^t=f_{ii}^t=4$.

A Klein bottle has attracted attention of researcher in many fields. We mention here, among the others, physics [13], where a considerable interest has emerged in studying lattice

models on non-orientable surfaces as new challenging unsolved lattice-statistical problems and as a realization and testing of predictions of the conformal field theory.

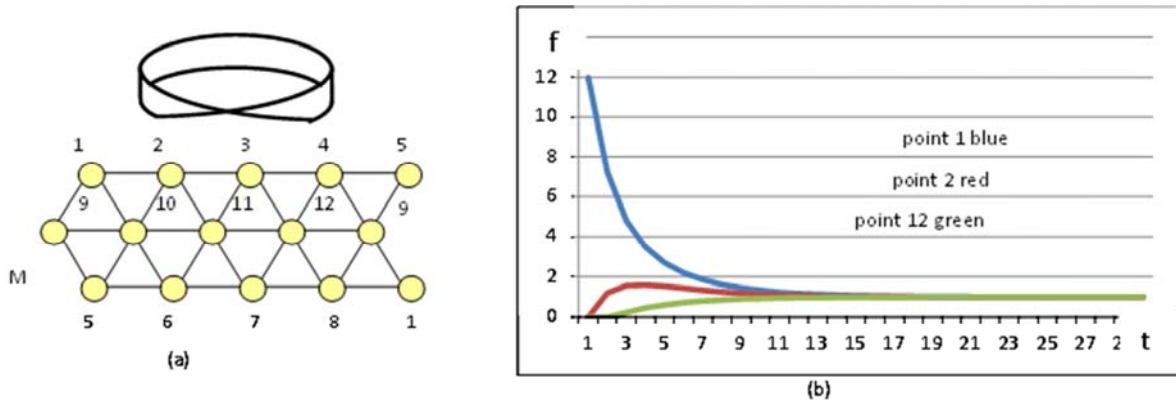


Fig. 9. (a) The Moebius strip M is formed by interior points 9, 10, 11, 12 and boundary points 1-8. (b) The solution profile of the initial value problem at points 1, 2 and 12 on the Moebius strip M , $t=0, 1, \dots, 30$, $f_1^0=12, f_k^0=0, k \neq 1$.

A digital Klein bottle K depicted in fig. 3 and fig. 7(a) consists of sixteen points. The rim $O(v_k)$ of every point v_k is a digital 1-sphere containing six points. K is a homogeneous digital space containing the minimal number of points. The number of points can be increased by using contractible transformation. Topological properties of a digital 2D Klein bottle are similar to topological properties of its continuous counterpart. For example, the Euler characteristic and the homology groups of a continuous and a digital Klein bottle are the same ([10] and [11]).

Define coefficients c_{pk} in the following way. If points v_p and v_k are adjacent then $c_{pk}=0.1$; $c_{kk}=0.4, k=1, \dots, 16$. Initial values are given as $f_1^0=16, f_k^0=0, k=2, \dots, 16$. In fig. 7(b), numerical solutions of the of the initial value problem for (20) are plotted at time $t=1, \dots, 100$. Two lines give the numerical solutions of the of the initial value problem for (20) at point 1 and point 3 (see fig. 7(a)). It follows from calculations that both lines converge to the same limit, $\lim_{t \rightarrow \infty} f_k^t = 1, k = 1, \dots, 16$. The physical interpretation of (20) on K is the heat equation and the numerical solution shows the temperature at points of K .

4.2. Digital 2D Projective Plane P . the Diffusion Equation on P

Fig. 2 shows a digital 2-dimensional projective plane P . P is a non-homogeneous digital space containing eleven points. The rim $O(v_k)$ of every point v_k is a digital 1-sphere. Topological properties of a digital and a continuous 2D projective plane are similar. It was shown in [10] and [11] that the Euler characteristic and the homology groups of a continuous and a digital projective plane are the same. It is easy to check directly that a digital 2D projective plane without a point is homotopy equivalent to a digital 1D sphere as it is for a continuous projective plane.

Define coefficients c_{pk} in the following way; if v_k and v_p are adjacent then $c_{kp} = c_{pk} = 0.1, c_{pp} = 1 - \sum_{k=1, k \neq p}^{11} c_{kp}$. Consider the numerical solutions of the initial value problem for (20). Initial values are given as $f_1^0=11, f_k^0=0, k=2, \dots, 10$. The profiles of the solution at points 1, 2 and 10 are plotted in fig. 8(a), where $t=1, \dots, 30$. It follows from direct calculations that all three lines converge to $b=1$. The physical meaning of these solutions is consistent with the distribution of particles on P caused by Brownian motion.

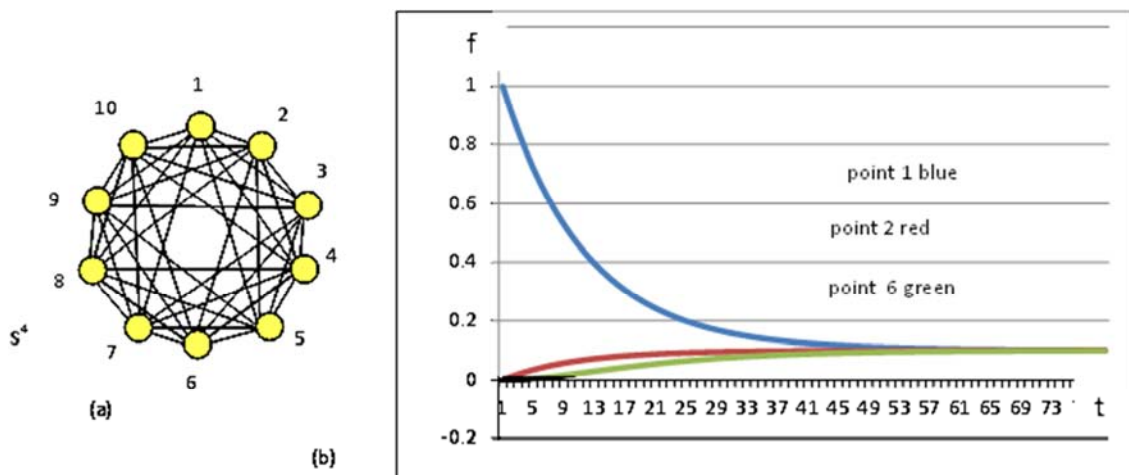


Fig. 10. (a) S^4 is a digital 4-dimensional sphere with ten point. (b) The solution profile of the initial value problem at point 1, 2 and 6 on S^4 , $t=0, 1, \dots, 80$, $f_1^0=1, f_k^0=0, k \neq 1$.

Consider the boundary value problem for (20). The boundary conditions are defined by equations $f_j^t=1, f_{11}^t=4$. Let $f_k^0=0, k=2, \dots, 10$. The profiles of the solution of the boundary value problem for (20) at points 2, 9 and 10 for $t=1, \dots, 30$ are shown in fig. 8(b).

This is consistent with the physical interpretation of (20) as heat equation, and the solution is the temperature distribution at points on P.

4.3. Digital 2D Moebius Strip M. the Heat Equation on M

The Moebius strip M depicted in fig. 9(a) consists of twelve points. This is the minimal possible number of points.

Points 9, 10, 11 and 12 are interior points, points 1-8 are boundary points which form a one-dimensional sphere (circle).

Assume that coefficients c_{ik} do not depend on t ; if $c_{ik} \neq 0, i \neq k$, then $c_{ik}=c_{ki}=0.1, c_{pp}=0.4, p=9, \dots, 12, c_{pp}=0.6, p=1, \dots, 8$. Initial values are given as $f_1^0=12, f_k^0=0, k=2, \dots, 12$. The profiles of the solution of (20) at points 1, 2 and 12 are shown in fig. 9(b), where $t=0, \dots, 30$. One may note that the difference between function values at different points dissipates with large passage of time. Direct computations show that $\lim_{t \rightarrow \infty} f_k^t = 1, k = 1, \dots, 12$. This is consistent with the physical interpretation of (20) as heat flow on M.

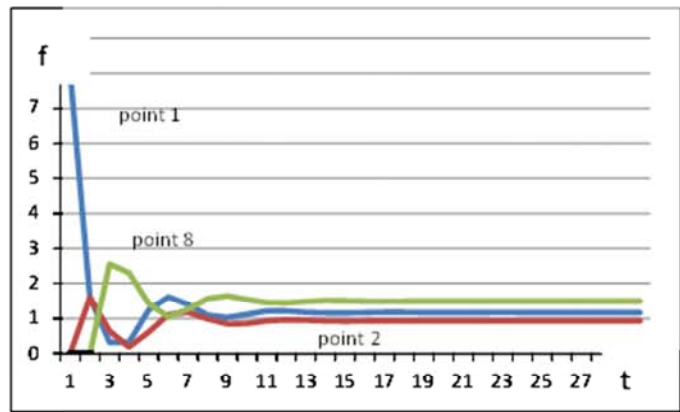
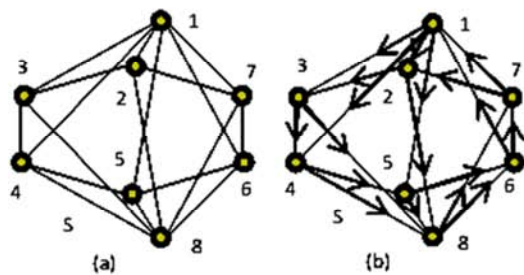


Fig. 11. (a) A digital 2D sphere S. (b) A directed network N on S. (c) The solution profile of the initial value problem at point 1, 2 and 8 on $S^d, t=1, \dots, 30, f_1^0=8, f_k^0=0, k=2, \dots, 8$.

4.4. Digital 4-dimensional Sphere S^4 . the Heat Equation on S^4

Consider a digital 4-dimensional -sphere S^4 with ten points depicted in fig. 4 and fig. 10(a). The rim $O(v_k)$ of every point v_k is a digital 3-sphere containing eight points and depicted in fig. 4. S^4 is a homogeneous digital space containing the minimal number of points. The number of points can be increased by using contractible transformation. Topological properties of a digital 4D sphere are similar to topological properties of a continuous 4D sphere.

Consider the numerical solutions of the initial value problem for (20). Let $c_{ik}=c_{ki}=0.01$ if points v_i and v_k are adjacent, and $c_{pp}=0.92$ for $p=1, \dots, 10$. Initial values are given as $f_1^0=1, f_k^0=0, k=2, \dots, 10$. The results of the solution of the initial value problem (20) at points 1, 2 and 6 for $t=0, \dots, 80$ are displayed in fig. 10(b), which illustrates the time behavior of the values of the function f . In the physical heat interpretation, this is the temperature distribution on S^4 . It follows from direct computations that $\lim_{t \rightarrow \infty} f_k^t = 0.1, k = 1, \dots, 10$.

4.5. Digital 2D Sphere S. A Directed Network

Consider a digital 2-dimensional sphere S with eight points depicted in fig. 11(a). The rim $O(v_k)$ of every point v_k is a digital 1-sphere. Define coefficients c_{pk} in equation (20) in

the following way; if $(v_i v_k) \in S$ then $c_{ik} > 0, c_{ki} = 0$ (or $c_{ik} = 0, c_{ki} > 0$), $c_{pp} = \sum_{k=1}^8 c_{kp}, p=1, \dots, 8$. In this case, equation (20) forms a directed network N on S shown in fig. 11(b). Edge $(v_i v_k)$ in S can be replaced with a directed edge (or arc) $(v_i \rightarrow v_k)$ from v_i to v_k . Dynamical system on such a network can be applied to a study of the movement of blood through the system of vessels or to an analysis of the of road traffic, ets. Let

$$c_{12} = c_{13} = c_{14} = c_{15} = c_{11} = c_{22} = c_{33} = c_{44} = c_{55} = c_{66} = c_{77} = c_{88} = 0.2, c_{21} = c_{28} = c_{34} = c_{38} = c_{45} = c_{48} = c_{56} = c_{58} = c_{67} = c_{61} = c_{72} = c_{71} = c_{86} = c_{87} = 0.4.$$

All other coefficients are equal to zero. Consider the numerical solutions of the initial value problem for (20). Initial values are given as $f_1^0=8, f_k^0=0, k=2, \dots, 8$. The results of the solution of (20) at points 1, 2 and 8 for $t=1, \dots, 30$ are displayed in fig. 11(c), which illustrates the time behavior of the values of the function. Dynamical system on such a network can be applied to a study of the movement of blood through the system of vessels or to an analysis of the of road traffic, ets.

5. A Method of Finding Numerical Solutions of a Parabolic PDE

Based on the results we presented in Sections 2 and 3, now we are able to describe a method that lets us find numerical

solutions of a parabolic PDE on, for example, a Klein bottle K .

Step 1. Construct a digital Klein bottle D with the necessary number of points defined by required accuracy and precision of the results.

Step 2. Determine appropriate coefficients c_{pk}^t in the parabolic PDE (6) on the digital D in accordance with continuous parabolic PDE on K .

Step 3. Compute the numerical solution of the parabolic PDE on D for a required t .

6. Conclusions and Open Question

A numerical explicit method for approximating the solution of differential parabolic equations on digital spaces, digital n -dimensional manifolds, $n > 0$, and networks is presented and some properties of this method are investigated. This method is mathematically correct in terms of digital topology in the comparison with other methods used before. Solutions of the equation on a digital Klein bottle, a digital projective plane, a digital 4D sphere, a digital Moebius strip and a directed network are presented.

An open question is to extend this method of solving parabolic PDE to other types of equations.

References

- [1] Gantmakher, F. R. (1959) The theory of matrices. New York, Chelsea Pub. Co.
- [2] Borovskikh, A. and Lazarev, K. (2004) Fourth-order differential equations on geometric graphs. *Journal of Mathematical Science*, 119 (6), 719–738.
- [3] Eckhardt, U. and Latecki, L. (2003) Topologies for the digital spaces Z^2 and Z^3 . *Computer Vision and Image Understanding*, 90, 295-312.
- [4] Evako, A. (2014) Topology preserving discretization schemes for digital image segmentation and digital models of the plane. *Open Access Library Journal*, 1, e566, <http://dx.doi.org/10.4236/oalib.1100566>.
- [5] Evako, A. (1999) Introduction to the theory of molecular spaces (in Russian language). Publishing House Paims, Moscow.
- [6] Evako, A., Kopperman, R. and Mukhin, Y. (1996) Dimensional properties of graphs and digital spaces. *Journal of Mathematical Imaging and Vision*, 6, 109-119.
- [7] Evako, A. (2006) Topological properties of closed digital spaces. One method of constructing digital models of closed continuous surfaces by using covers. *Computer Vision and Image Understanding*. 102, 134-144.
- [8] Evako, A. (2015) Classification of digital n -manifolds. *Discrete Applied Mathematics*. 181, 289–296.
- [9] Evako, A. (1995) Topological properties of the intersection graph of covers of n -dimensional surfaces. *Discrete Mathematics*, 147, 107-120.
- [10] Ivashchenko, A. (1993) Representation of smooth surfaces by graphs. Transformations of graphs which do not change the Euler characteristic of graphs. *Discrete Mathematics*, 122, 219-233.
- [11] Ivashchenko, A. (1994) Contractible transformations do not change the homology groups of graphs. *Discrete Mathematics*, 126, 159-170.
- [12] Lankaster, P. (1969) Theory of matrices. Academic Press, New-York-London.
- [13] Lu, W. T. and Wu, F. Y. (2001) Ising model on nonorientable surfaces: Exact solution for the Moebius strip and the Klein bottle. *Phys. Rev.*, E 63, 026107.
- [14] Pokornyi, Y. and Borovskikh, A. (2004) Differential equations on networks (Geometric graphs). *Journal of Mathematical Science*, 119 (6), 691–718.
- [15] Smith, G. D. (1985) Numerical solution of partial differential equations: finite difference methods (3rd ed.). Oxford University Press.
- [16] Vol’pert, A. (1972) Differential equations on graphs. *Mat. Sb. (N. S.)*, 88 (130), 578–588.
- [17] Xu Gen, Qi. and Mastorakis, N. (2010) Differential equations on metric graph. WSEAS Press.